Orbital Angular Momentum Mode Intelligent Identification in the Secondary Frequency Domain with Compressive Sensing

Chao Zhang, Jin Li, Yuanhe Wang

School of Aerospace Engineering, Tsinghua University, China
zhangchao@tsinghua.edu.cn, j-i17@tsinghua.org.cn, wang-yh19@mails.tsinghua.edu.cn

Abstract

The Electro-Magnetic (EM) waves with Orbital Angular Momentum (OAM) can achieve the high spectral efficiency by multiplexing different OAM modes. In order to effectively identify the OAM modes received in the partial phase plane, different modes are mapped to the frequency shifts in the secondary frequency domain. The high-speed acquisition equipment is necessary for the traditional method in the process of receiving Radio Frequency (RF) or Intermediate Frequency (IF) signals, which suffers from a high cost. However, Compressive Sensing (CS) can break the Nyquist sampling restriction by random observation and is expected to build the relationship between the received signal and the frequency shift in the secondary frequency domain at a lower sampling rate, so that the cost is low. Moreover, due to the existence of the multipath effect, the transfer learning is employed to establish the spectrum-mode mapping, which further improves the Bit Error Rate (BER) performance and the transmission distance. Therefore, this paper proposes an intelligent OAM mode identification method based on CS and transfer learning. Meanwhile, the random sampling is carried out based on the Analog-to-Information Converter (AIC) to realize the OAM mode identification with the low sampling rate. The simulation results can verify the validity and efficiency of this method.

Keywords: Orbital angular momentum, Secondary frequency domain, Compressive sensing, Analog-to-information converter, Intelligent mode identification

1 Introduction

As an intrinsic property of the Electro-Magnetic (EM) waves, Orbital Angular Momentum (OAM) is considered as the new dimension of wireless transmission, especially in future mobile communications. Due to the orthogonality between different OAM modes, they can be multiplexed to achieve the higher spectral efficiency and transmission rate, which makes OAM an important development direction of Beyond 5th Generation (B5G) and 6th Generation (6G) mobile communications in the future [1-2]. Furthermore, OAM can not only increase the capacity by multiplexing, but also improve the transmission performance by Index Modulation (IM) [3]. However, the non-zero divergence angle is caused by the inverted cone shaped beams and the spiral phase distribution. When propagating in the free space, the divergence of the non-zero beam angle results in the increasing of the circular energy ring radius in the transverse plane, which makes it difficult to receive the all-phase plane in a long-distance transmission [4]. Therefore, the partial phase plane reception for OAM must be considered.

For the partial phase plane receiving method [5], when different non-degenerate OAM modes are used to multiplex EM waves, the one-to-one frequency shift can be mapped to the secondary frequency domain by Virtual Rotating Antenna (VRA) [4, 6], so as to realize the accurate identification of OAM modes. In Dec. 2016, the 27.5 km EM wave OAM transmission experiment was successfully completed [7-8]. In Apr. 2018, the same research team also completed a 172 km ground-to-air transmission experiment from Beijing to Xiongan New Area in the north of Hebei Province, China [9]. However, with the coming of big data and internet of things [10-12], in the future B5G and 6G, due to the limited sampling capability of our existing hardware devices, it is difficult to meet the requirement of the high transmission rate, e.g. Tbps. Even if the high sampling rate can be achieved, the cost is huge. Therefore, in order to reduce the sampling rate, how to build the relationship between the received signal and the frequency shift in the secondary frequency domain so as to identify the OAM mode? It has become a difficult problem confronting us.

As a new sampling theory, the Compressive Sensing (CS) takes advantage of the sparse characteristics of the signal and uses the random sampling to obtain the discrete samples of the signal under the condition of the far less than Nyquist sampling rate [13-14]. Moreover, It can realize the perfect recovery of the signal through the non-linear reconstruction algorithm

*Corresponding Author: Chao Zhang; E-mail: zhangchao@tsinghua.edu.cn
DOI: 10.3966/160792642020112106016

[15-16]. In recent years, CS theory has been applied to the detection of Generalized Space Shift Keying (GSSK) symbols in the uncertain Multiple-Input Multiple-Output (MIMO) transmission systems with the better performance [17], such as Orthogonal Matching Pursuit (OMP) [18] and the Basis Pursuit (BP) [19]. In addition, in the wake of the related research of the Analog-to-Information Converter (AIC) with Limited Random Sequence (LRS) modulation [20], the required sampling rate may be further reduced.

In addition, even if the relationship between the received signal and the frequency shift in the secondary frequency domain can be established, due to the multipath effect in the transmission channel, the position and amplitude of the frequency shift in the secondary frequency domain are indirectly affected. That will make the mapping relationship between the frequency shift and the OAM mode unknown, which in turn affects the identification of OAM modes. The Convolution Neural Network (CNN) method has already been proposed as the effective method to achieve task learning [21], target recognition [22-23], channel estimation [24], signal detection [25], which can be used to determine the active OAM modes in the transmitted signal [26-28]. Nevertheless, in the process of identification, the problems of over-fitting and low detection accuracy often arise because of the limited number of datasets. Therefore, the CNN method cannot be directly used for training and it is necessary to migrate the pre-trained CNN model, share the parameters of the corresponding convolution layer and the pool layer, and adjust the hyperparameters [29], which obtains good performance. Thus, the transfer learning has emerged as a new learning framework that may achieve this goal [29].

In this paper, the CS and the transfer learning are applied to nondegenerate OAM multiplexing transmissions. Using AIC with LRS modulation as a detector through random sampling [20], the low sampling rate with CS can be used to build the model of the received signal and the frequency shift in the secondary frequency domain. Besides, the transfer learning is employed to establish the spectrum-mode mapping, thus accurately identifying OAM modes, and then the high-speed transmission will be achieved. Notably, the method proposed in this paper can effectively solve the major problems, i.e., the innovations can be highlighted as: (1) When sampling Radio Frequency (RF) signals directly, the sampling rate is very high, which makes the hardware equipment expensive. Besides, if analog devices are utilized to down-convert the RF signals received by antennas and then sample them at Intermediate Frequency (IF), the phase error and attenuation will be caused, which seriously affects our identification accuracy of OAM modes. Simultaneously, the sampling rate of the employed data acquisition card limits the data rate of the high-speed transmission; (2) At low sampling rates, the relationship between the received signal and the frequency shift in the secondary frequency domain is unknown; (3) The existence of multipath channel puts a negative effect on the identification of OAM mode, which limits the Bit Error Rate (BER) performance and the transmission distance.

The rest of the paper is organized as the following. Section 2 provides an overview of the traditional methods. Compared with the shortcomings of the traditional methods, the system architecture of the method proposed in this paper is given in Section 3. Section 4 establishes the mapping relationship between the received signal, the spectrum and the OAM mode in the secondary frequency domain. Moreover, Section 5 gives some simulation results to verify the validity and efficiency. Finally, Section 6 concludes the paper and further looks forward to the development in the future.

2 Preliminary Knowledge

In the previous work, a method of detecting OAM by the partial phase plane reception using VRA interpolation was proposed [7]. Receiving OAM wave using the VRA can generate the rotational Doppler frequency shift, and the frequency shift in the corresponding transform domain will arise by the interpolated signals received by the antennas. In this transformation domain, different index keying sets bring the different OAM modes combinations, and different OAM modes combinations will produce the different frequency shifts, but only one spectrum line will be obtained. Because it has the same physical dimension as the traditional frequency domain, the transformation domain that produces the frequency shifts is named as the secondary frequency domain [6]. Generally, the “first” frequency domain can be considered as the traditional frequency domain.

In this process, the multiple combinations of different non-degenerate OAM modes are converted into the same frequency signal but with different frequency shift combinations, which realizes the demodulation and identification of multiplexed OAM modes. Based on VRA, there are two commonly used receiver structures based on RF and IF sampling, as shown in Figure 1. Specifically, in Figure 1(a), the high-speed sampling oscilloscope at the receiving end oversamples directly the RF signal, and then different OAM modes are converted into the frequency shifts by VRA, which can be used for the offline detection of OAM modes. Because of the high sampling rate requirement, the cost of this method is very high.

In contrast, in Figure 1(b), the RF signal obtained by the receiver is down-converted to IF. Then, the OAM mode can be identified in real time by the low-rate data acquisition card. However, due to the low sampling rate hardware limitation, this method will restrict the bandwidth of the IF frequency, thus reducing the

amount of data carried by the IF bandwidth.

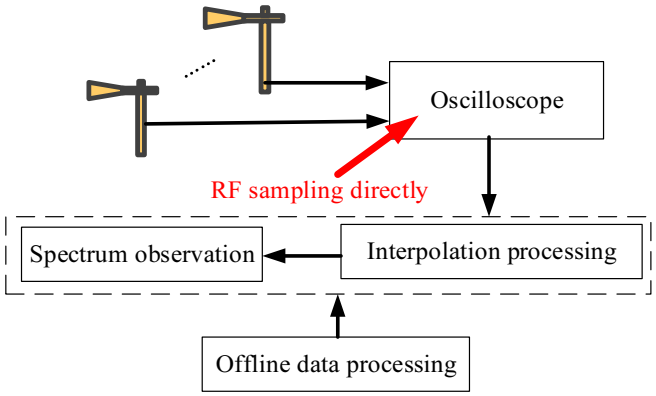

(a) Receiver with oscilloscope

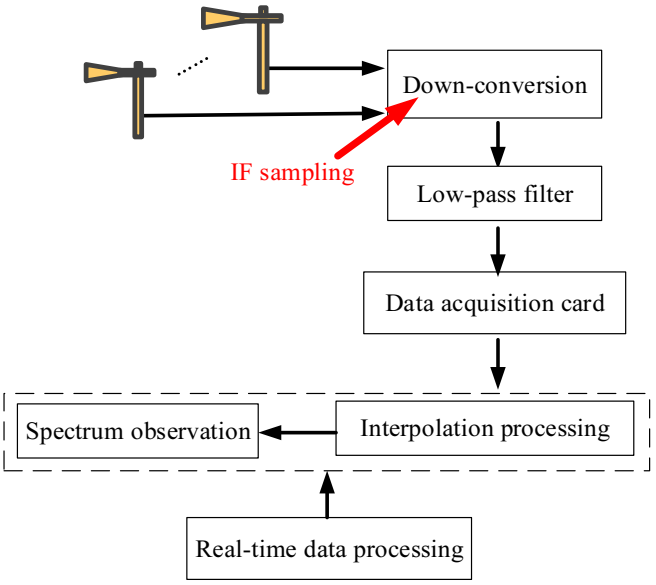

(b) Receiver with down-conversion

Figure 1. The comparison of receiver structures based on RF and IF sampling

In summary, the traditional RF and IF receiver of OAM waves are based on the Nyquist sampling theorem. At present, there is no research on the use of CS in the identification of OAM mode under the premise of the low sampling rate. Besides, due to the multipath effect, the model between the frequency shift in the secondary frequency domain and the OAM mode is unknown, which brings the direct difficulty to identify the OAM modes.

3 System Architecture

3.1 System Structure

As we know, CS algorithm can break the Nyquist sampling rate. Because of the limitation of hardware resources, CS algorithm combined with the low sampling rate AIC is used to effectively replace the high-speed sampling oscilloscope, which greatly reduces hardware cost. On the other hand, when reducing the sampling rate required by the hardware, a model of the received signal and the frequency shift in the secondary frequency domain should be established.

Specifically, the RF signals received by antennas are randomly sampled by AIC, and the spectrum line mapped to OAM mode is separated and recovered in the secondary frequency domain by CS, which greatly improves the data transmission rate and avoids the cost of the high-speed sampling device.

In addition, the transfer learning is helpful to establish the spectrum-mode mapping and realize the OAM mode identification within the multipath environment, which can be employed instead of the traditional method, such as Maximum Likelihood Estimation (MLE). Figure 2 illustrates the receiver with AIC, CS algorithm and transfer learning modules.

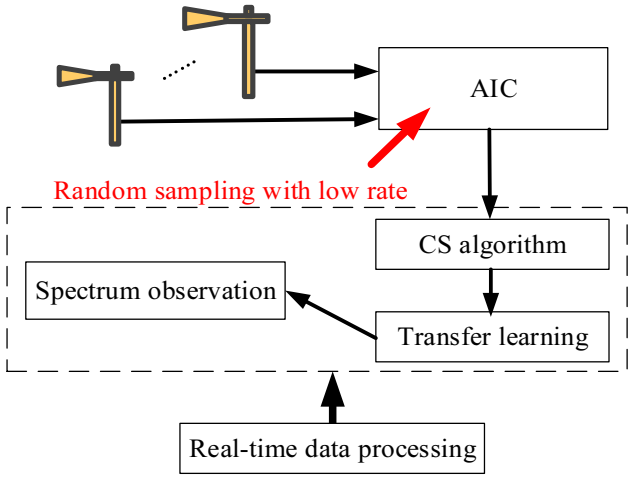

Figure 2. The receiver structure with AIC, CS algorithm and transfer learning modules

3.2 Analog-to-Information Converter

In this subsection, a promising symbol detector with the random sampling is reviewed. AIC with LRS modulation is adopted at the receiving end, and the structure of AIC with LRS modulation is shown in Figure 3. It consists of the limited random sequence, integrator and low-power Analog-to-Digital Converter (ADC). Unlike the traditional ADC, AIC can sample signals randomly. The LRS elements are composed of "1" and "0". By mixing the sequence of "0" and "1" and integrating the mixed signal, the physical process of the random sampling is completed well by the sampler. Assume the sequence is in length N and consists of M frames, and each frame is in length L. The elements are composed of N - 1 "0" and only one "1", and the location of "1" is random [20]. Assume that the position of "1" is q, where q is a random integer between 0 and L – 1, and the generation of random integer follows a distribution, such as a uniform distribution.

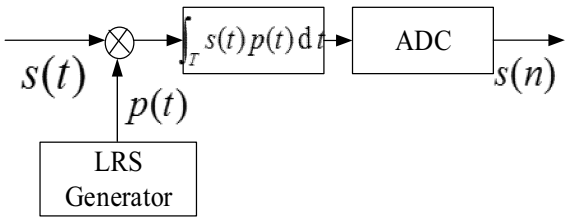

Figure 3. The structure of AIC with LRS modulation

The input signal $s(t)$ and the signal $p(t)$ generated by the periodic transmission of a finite length random sequence are mixed, and the mixing results are fed into the integrator, where the period of the integrator is the reciprocal of the average sampling rate of the random sampler, and then the integrator is connected to the traditional ADC. In the sampling process, only when the integrator and ADC are synchronized with the finite length sequence generator, can the random sampling of the analog signal be realized. The output $s(n)$ is a discrete signal, which will be sent to the successive real-time data processing module by CS algorithm for recovery.

Overall, if the number of the original sampling points is N, then after the AIC with LRS modulation, the ADC can use the sampling points number of M for sampling, and M is generally much smaller than N.

3.3 Compressive Sensing Algorithm

The CS technology breaks through the limitation of the uniform sampling rate in the traditional Nyquist sampling theorem. For sparse signals, the random sampling is used to recover the complete signal with the sampling rate far less than the Nyquist sampling rate [15-16].

Since the random sampling of AIC at the receiver can meet the requirement of CS, the OAM modes with a known sparsity can be identified by CS algorithm. For CS algorithm, there are two kinds of widely used greedy algorithms: Matching Pursuit (MP) algorithm and Orthogonal Matching Pursuit (OMP) algorithm.

When the measurement matrix is not easy to obtain, MP algorithm can use the greedy iteration algorithm to construct a matching dictionary and obtain sparse vectors. Compared with MP algorithm, the improvement of OMP algorithm is based on the Schmidt orthogonalization of the selected columns in each iteration to accelerate the convergence of the algorithm. For OAM mode identification, the measurement matrix is known and the real-time demodulation needs to be guaranteed. Thereby, this paper considers and employs the OMP algorithm [30].

3.4 Transfer Learning

It is well known that Artificial Intelligence (AI) extracts features from training data, summarizes, integrates and adjusts the accuracy of the model gradually [31], but the process is based on the assumption that: the same distribution of the training data and the test data. When the distribution changes, most statistical models need to be rebuilt with the newly collected training data, but this is not realistic. In such case, the transfer learning between task domains is desirable.

Concerning the multipath channel in the actual transmission, the channel model is difficult to be estimated, and the transfer learning as a new AI method is proposed. It mainly includes the pre-training process of CNN into the source domain datasets and the later learning process of the target domain datasets with the mode migration, in which the target domain is set to identify OAM modes. In the case of the high SNR, the two-dimensional line image is mapped to OAM mode in the secondary frequency domain after VRA interpolation algorithm, which needs to be transferred for learning training. Ideal secondary frequency spectrum is a single line in the time invariant location. However, due to the multipath transmission, the spectrum line is time variant for the same OAM mode. For OAM mode datasets, the input is the position and amplitude of the spectrum line in the secondary frequency domain and the output is OAM mode number. In the actual OAM mode multiplexing long distance transmission, the OAM mode needs to be determined first, so that the demodulation can be achieved. When the data at the low sampling rate are received, the spectral lines in the secondary frequency domain need to be reconstructed through the CS algorithm. However, if the receiving terminal has mobility, such as an on-board mobile receiving station, the channel simultaneously shows time varying characteristics. Then according to the position and amplitude information of the spectral lines after CS, the OAM mode must be identified through transfer learning.

Since the ImageNet datasets cover 1.2 million images, it has been widely used for the training of universal models. Therefore, due to the few OAM mode datasets in the target domain, for the migration pre-training process, the CNN model AlexNet after the training of ImageNet datasets is adopted [32].

Firstly, the original AlexNet model is a classification task for 1000 categories, so the last three layers must be emphasized and re-adjusted, i.e., a connection layer, a softmax layer, and a classification layer should be replaced. Secondly, adjust the parameters of the fully connected layer. In order to accelerate the training process, the value of the weight coefficient and offset bias can be increased. Thirdly, set hyperparameters, i.e., reduce the initial learning rate, slow down the learning of the transfer layer, and speed up the training of the last three layers. Finally, modify the output layer to the size of the OAM mode number, and initialize the output layer weight. Notably, the transfer learning hyperparameters are listed in Table 1.

Table 1. Transfer learning parameters

Training parameters	Value
Learning rate	0.01
Learning attenuation	0.001
Momentum	0.5
Weight attenuation	0.005
Batch size	64

The detailed process of the fine tuning is shown in Figure 4. Initially, all weights are initialized. Afterwards, some parameters are fine tuned to reduce the learning rate, and then the training is carried out according to the new datasets of OAM mode. Consequently, OAM modes can be identified with the high precision, and the index key combination of the corresponding modes can be obtained.

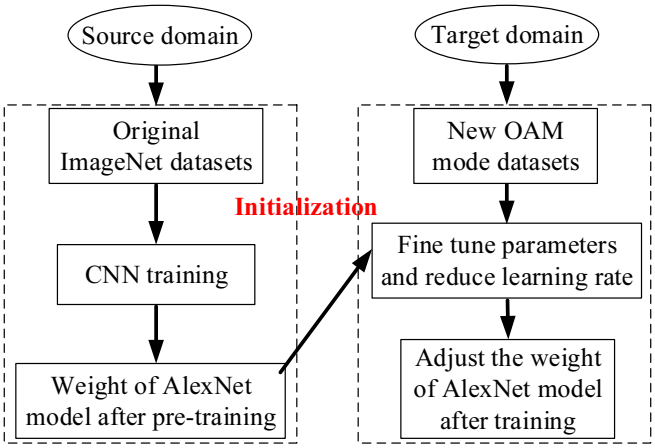

Figure 4. Fine tuning process

It should be emphasized that the fine tuning process is based on the AlexNet model weight after CNN training of the original ImageNet datasets in the source domain [32]. In the target domain, some training parameters are fine tuned according to the new OAM mode datasets, mainly including the learning rate and the batch size.

4 Mathematical Model

According to Figure 3, the signal through AIC with LRS modulation can be denoted as follows

$$s(n) = \int_T s(t)p(t)\mathrm{d}t. \tag{1}$$

It is well known that the recovery process of OMP is to reconstruct the P-dimensional original signal $\mathbf{z}$ from the known Q-dimensional measurement signal $\mathbf{s}$ and the measurement matrix $\mathbf{\Phi}$. Assuming that the length of the signal $\mathbf{z}$ is P, it is sparse under a projection array $\mathbf{\Psi}$, $\mathbf{\Psi}$ is the $P \times P$ matrix, only K elements are greater than the threshold ϵ, where K is far less than P, the measured value can be obtained by observing the signal $\mathbf{z}$ on the basis $\mathbf{\Phi}$, $\mathbf{\Phi}$ is the $Q \times P$ matrix, then we can get

$$\mathbf{s} = \mathbf{\Phi z} = \mathbf{\Phi \Psi f} = \mathbf{\Theta f}, \tag{2}$$

where, $\mathbf{\Theta} = \mathbf{\Phi \Psi}$, $\mathbf{\Theta}$ is the sparse representation of the signal, $\mathbf{f}$ is the spectrum in the secondary frequency domain. The dimension Q of the measured value in the above Equation (2) is less than the dimension P of the signal. There are infinite solutions to the equation. It needs exhaustive time to search the correct result. However, this problem can be efficiently solved in the method with minimum norm problem.

Since LRS sequence can satisfy the random sampling requirement of OMP algorithm, OMP algorithm is considered to recover the spectrum line in the secondary frequency domain according to the signal after AIC with LRS. Thus, according to [7], receiving an OAM wave using the VRA can generate the interpolated signals, and rotational Doppler frequency shift can be detected from the interpolated signals. Based on that, the measurement matrix $\mathbf{\Phi}$ can be defined as

$$\mathbf{\Phi} = \mathbf{w}^{\mathrm{T}} = \mathbf{P}^{\mathrm{T}}\mathbf{R}^{-\mathrm{T}}, \tag{3}$$

where $\mathbf{w}$ is the matrix of the weighting coefficient for the received signal after AIC, $(\cdot)^{\mathrm{T}}$ denotes the transpose of the matrix, $\mathbf{P}$ is the cross-correlation matrix between the received signal and the interpolated signal, and $\mathbf{R}$ is the autocorrelation matrix of the received signal.

Then, according to the measurement matrix $\mathbf{\Phi}$ and the received signal $\mathbf{s}$, the frequency shift of the interpolation signal can be obtained, which is the spectrum $\mathbf{f}$ in the secondary frequency domain.

The spectrum lines in the second frequency domain can be obtained by OMP algorithm based on the measurement matrix, and the channel matrix from the transmitter to the receiver in the free space can be obtained easily [33-35]. Considering that the channel model is multipath in the actual transmission, the position and amplitude of the spectrum lines in the second frequency domain are affected, which subsequently changes the ways of the OAM mode identification. The position and amplitude of the spectrum $\mathbf{f}$ can be defined

$$\mathbf{f} = (A, \omega) = f(\mathbf{H}_{\mathrm{OAM}}), \tag{4}$$

where, A, ω indicate the amplitude and position of the secondary frequency spectrum respectively, $\mathbf{H}_{\mathrm{OAM}}$ represents the multipath model of OAM channel, $f(\cdot)$ is a mapping relation function.

Due to the time variant property of the spectrum line in the secondary frequency domain, it's necessary to introduce intelligent method to help us realize the mapping relation between the spectrum line and the OAM mode.

Compared with L_2 norm, L_1 norm makes the transfer learning converge faster, therefore L_1 norm is used as the criterion [24]. Then, the final model needs to

minimize the L_1 norm of the source AlexNet model and the target spectrum-mode mapping model.

$$L_1 = \left\| \mathbf{\Omega}_t - \Gamma \mathbf{\Omega}_s \right\|_1, \tag{5}$$

where, $\| \ \|_1$ denotes the one norm for the vector, $\mathbf{\Omega}_s$ is the source AlexNet model, $\mathbf{\Omega}_t$ is the target spectrum-mode mapping model, Γ controls the transfer regularization amount. Moreover, in order to regularize the distance between the target spectrum-mode mapping model and the learned AlexNet model [36], the target spectrum-mode mapping domain weight parameters must be trained again. Thus, the objective function used in this paper can be expressed as

$$J = \min_{\mathbf{\Omega}_t} \left\| \mathbf{\Omega}_t - \Gamma \mathbf{\Omega}_s \right\|_1 + C \sum_{i=1}^{N} [l_i - \mathbf{\Omega}_t(\mathbf{f}_i)], \tag{6}$$

where, C controls the weight of the loss function, l_i denotes the i-th OAM mode output, $\mathbf{f}_i$ is the i-th spectrum in the secondary frequency domain, N is total number of OAM training datasets.

5 Performance Evaluation

5.1 The Comparison of Receiver Structure

According to the description in Section 3 and Section 4, an example is proposed to show the validity of the proposed method. Additionally, in order to further analyze the efficiency, we compare the identification probability, the Bit Error Rate (BER) performance and the capacities in three cases, i.e., the cases of RF sampling directly, IF sampling and OMP with AIC.

5.1.1 Example

The main simulation parameters are listed in Table 2 and results are all conducted with MATLAB R2016a programming platform. Assuming that the separated OAM Mode 1 and OAM Mode 2 are generated for index keying transmission at the transmitter respectively, and the 100 MHz IF signal is up-converted to 10 GHz RF, fed to the Uniform Circular Array (UCA) composed of 16 array elements, then received by two antennas placed at the receiving energy ring through the partial phase plane method at the receiver. The receiver will restore the spectrum lines according to the index keying set of the different OAM mode combinations. Figure 5 illustrates the signals received by Antenna 1 and Antenna 2 for OAM Mode 1, and Figure 6 shows the signals received by Antenna 1 and Antenna 2 for Mode 2.

The limited random sequence $p(t)$ designed is shown in Figure 7. The length of the signal is 128, and consists of 16 frames, each frame is in length 8. Then, the measurement signals utilized by CS for OAM Mode 1 after AIC with LRS can be shown in Figure 8, and the measurement signals used by CS for OAM

Table 2. Simulation parameters

Parameters	Value
Carrier frequency	10 GHz
Signal length	128
Modulation scheme	QPSK
Beam divergence angle	2°
UCA radius	9 cm
Array element number	16
Receiver ring radius	3.49 m
Receiving antennas space	1 m
Transmission distance	100 km
OAM modes	1, 2
Sampling rate	1.25 GHz

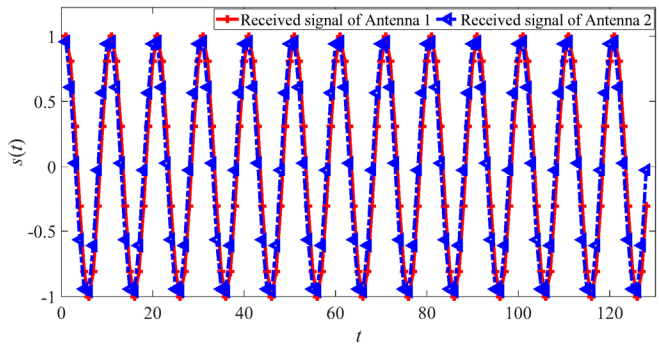

Figure 5. Received signals of Antenna 1 and Antenna 2 for Mode 1

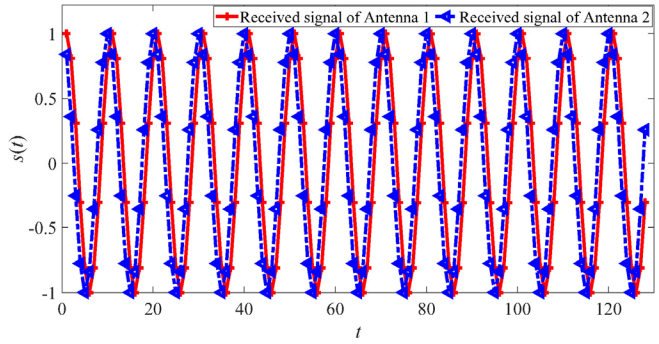

Figure 6. Received signals of Antenna 1 and Antenna 2 for Mode 2

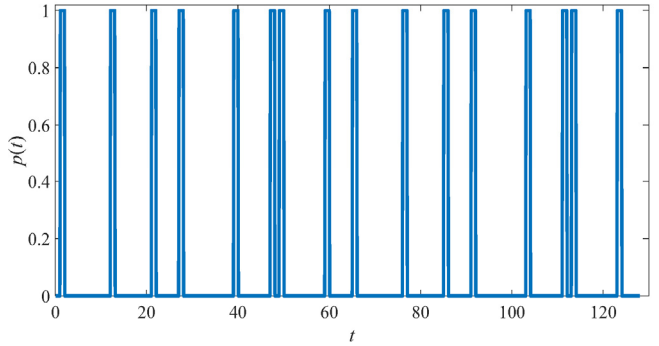

Figure 7. Typical figure of the LRS $p(t)$

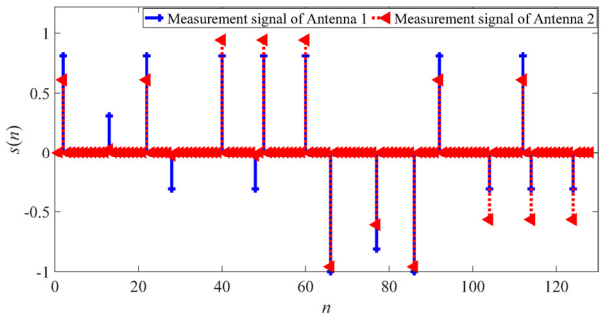

Figure 8. Typical measurement signals used by CS for Mode 1 after AIC

Mode 2 after AIC with LRS can be shown in Figure 9. Both low-rate measurement signals will be applied to recover the spectrum line in the secondary frequency domain.

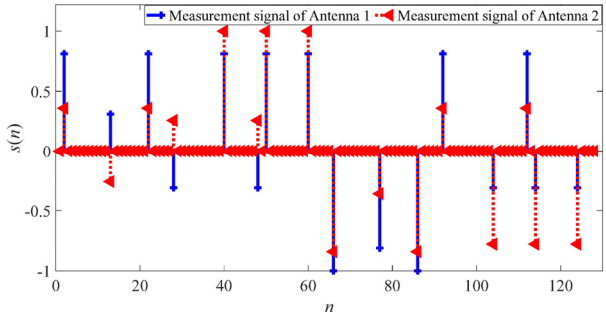

Figure 9. Typical measurement signals used by CS for Mode 2 after AIC

According to the known sparsity of "1" and the measurement signals, the reconstruction is carried out by combining the OMP algorithm. Finally, the recovered signal can be converted to a spectrum line in the secondary frequency domain, so that the separated Mode 1 and Mode 2 are converted to the frequency shift in the secondary frequency domain respectively. As shown in Figure 10, the index of the different OAM modes will be obtained based on the different frequency shifts. Moreover, it should be noted that this example covers only two cases in the index keying combination of OAM Mode 1 and Mode 2. Certainly, there are also cases where neither two OAM modes are sent and both OAM modes are sent, and the process is similar. Besides, if the mixed multiple OAM modes are sent at the same time, the spectrum is only a single line.

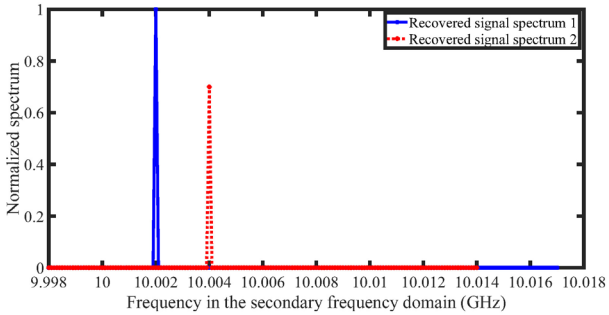

Figure 10. Spectrum in the secondary frequency domain

As we know, if the Nyquist sampling is used, two sampling points at least are required for each signal period. Then, for this example, there are at least 26 sampling points. However, 16 sampling points have been used to realize the low-rate sampling of 10 GHz RF signal and reconstruct the spectrum line in the secondary frequency domain, so that OAM mode identification is achieved. Thus, the method of AIC with CS proposed in this paper has been verified.

5.1.2 Analysis

Comparison of analog devices. Traditional RF receiver of OAM waves is based on the Nyquist sampling theorem. For example, if 10 GHz RF signal is sampled, a sampling rate of at least 20 GHz is required. In practice, more than 2 points need to be taken in a sampling period in order to recover the signal well. The cost of such a high sampling oscilloscope is extremely higher than the method of IF sampling and OMP with AIC. What's more, if the down-conversion is adopted, the sampling rate of the data acquisition card is up to 1.25 GHz, which limits the bandwidth of IF. However, due to the requirement of the low sampling rate, the higher bandwidth can be obtained through OMP with AIC compared with IF sampling, and then the higher data transmission rate can also be achieved.

Simulation results. Figure 11 demonstrates that when SNR increases, the identification probability P_{I} increases quickly. It can be noted that when the SNR reaches about 19 dB, the identification probability of the proposed method in this paper will approach 1, which is superior to the traditional IF sampling. The lower the out-of-band interference ratio I_{B} is, the higher the identification probability of OAM is. Besides, if I_{B} is as low as 0.001, the identification probability of IF sampling is very close to that of RF sampling and OMP with AIC. Especially, when P_{I} is greater than the threshold probability $P_0 = 0.89$, this method will work well.

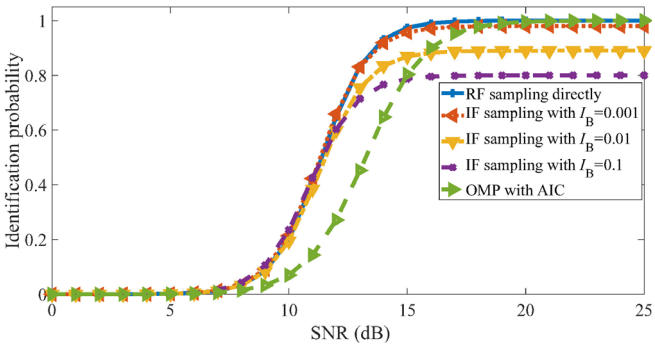

Figure 11. Identification probability varying with SNR

According to the identification probability P_{I}, the BER denoted by P_{BER} can be obtained as

$$P_{\mathrm{BER}} = 1 - P_{\mathrm{I}} \tag{7}$$

Therefore, the BER simulation is shown in Figure 12, the highest BER performance of IF sampling can be found under certain SNR, and the BER performance of OMP with AIC is fairly better than IF sampling.

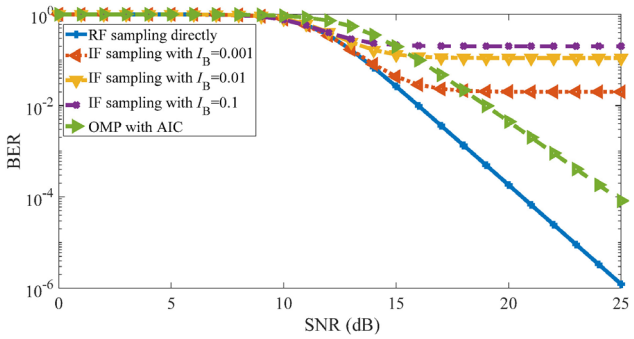

Figure 12. BER simulation result

For a communication system, the transmission capacity is also an extremely important evaluation indicator. Consequently, Figure 13 illustrates the capacity curve as BER changes according to the Shannon formula and BER curve. The capacity curve of OMP with AIC is close to the RF sampling directly.

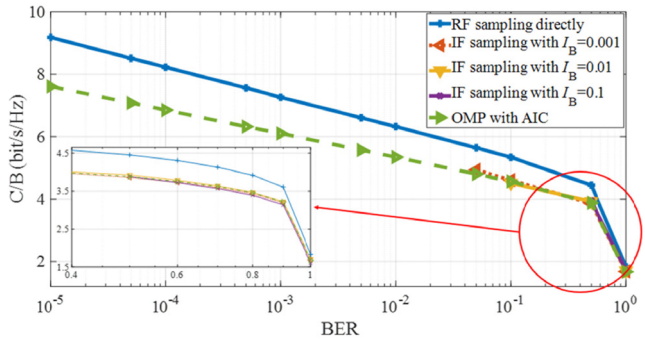

Figure 13. Capacity comparison

Overall, OMP with AIC is able to be used for random sampling at a fairly low sampling rate, which is of great benefit to replace the high-speed sampling scheme. However, the sampling equipment with AIC increases the difficulty. Then, the trade-off should be considered in the practical application.

5.2 The Comparison of Establishing Spectrum-Mode Mapping after CS

5.2.1 Generation of Training Datasets

Multipath effect is that when EM wave is transmitted in free space, multiple paths signals are generated due to the reflection or scattering, and different paths arrive at the receiving end at different times. If they are superimposed, the interference or even fading will occur, which affects the original signal receiving and even makes errors.

We will artificially build the training datasets. Suppose that a sinusoidal signal with a single frequency of 10 GHz and an amplitude of 1 is generated. This sinusoidal signal carries different initial phases that correspond to different OAM modes, and the amplitude fading is set to 0.8. The time delay is 20 random numbers. Then, the 20 paths can be superimposed, and Additive Gaussian White Noise (AWGN) is added to generate an array of length 1000 and 1000 groups. After VRA, the positions and the amplitudes of the different spectrum lines in the secondary frequency domain are obtained respectively, but the corresponding mode is the same. The process for other modes is similar. Notably, OAM Mode 1 is used as an example. Through a large number of repeated tests, if the single identified mode is between 0.5 and 1.5, the experimental test is believed to identify the OAM mode correctly.

Due to the existence of the multipath channel in the actual transmission, some intelligent methods must be considered.

The multipath effect transmission scenario is shown in Figure 14, the ellipsis indicates multiple paths.

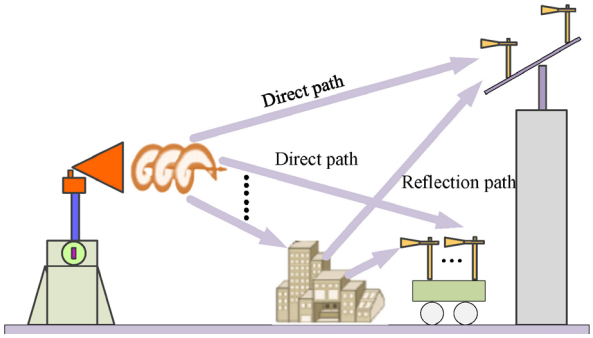

Figure 14. OAM transmission scenario under the multipath effect

Hence, in order to analyze the validity and efficiency of the transfer learning method used in channel estimation, the identification probability, Bit Error Rate (BER) and capacity are compared with three cases, i.e., Back Propagation (BP) neural network, CNN and the traditional MLE method. The experimental environment configuration is based on Matlab development environment equipped with i7 (main frequency 3.2 GHz, quad-core) with 8GB memory. Besides, the number of datasets generated under different SNR is 15,000 in total, and the training time required is nearly 2 hours and depends on machine configuration. The detailed simulation parameters are shown in Table 3.

Table 3. Simulation parameters

Parameters	Value
Carrier frequency	10 GHz
Signal bandwidth	70 MHz
Modulation	QPSK
Receiving antenna spacing	1 m
Transmission distance	100 km
Learning rate	0.002

5.2.2 Identification Probability

Because the transfer learning is aimed to make full use of the trained AlexNet model of million datasets to fine tune some parameters, the model has achieved good results on limited number of OAM datasets. As shown in Figure 15, when SNR increases, the identification probability P_I increases. It can be seen that when the SNR is in the range of 5-15 dB, the identification probability of the transfer learning is far greater than that of BP neural network, CNN and the traditional MLE method, which greatly improves the performance of OAM mode identification.

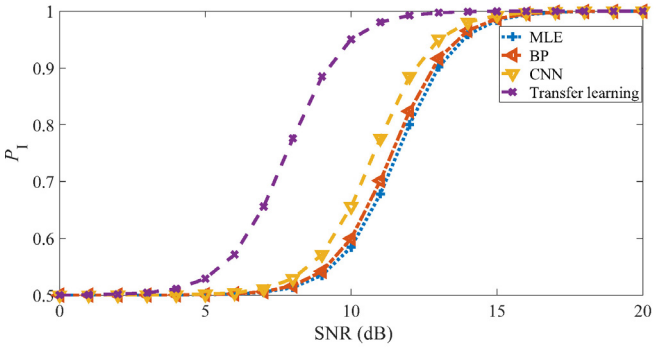

Figure 15. Identification probability varying with SNR

5.2.3 BER

According to the identification probability and Equation (7), the BER curve is shown in Figure 16. It can be found that the traditional MLE has similar BER with BP neural network and CNN, but the BER curve of the transfer learning is far lower than those three methods. Under the same BER, the best SNR gain can be increased by 4 dB, which leads to that the transmission distance can be extended from 100 km to 158.4 km. Otherwise, in the case of the same distance, the sensitivity is improved, i.e., the minimum required SNR in the receiver is reduced.

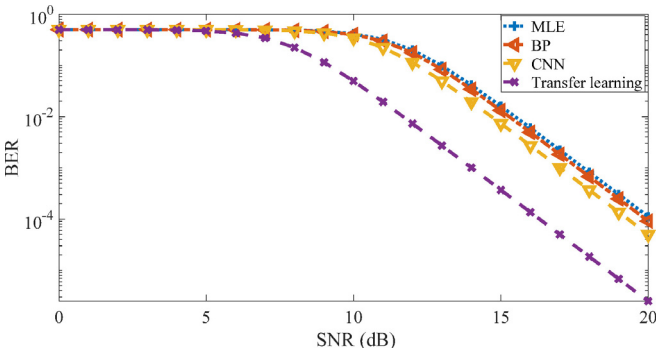

Figure 16. BER simulation results

6 Conclusion

The proposed intelligent method in this paper, which combines CS algorithm with the low sampling rate AIC, has been effectively applied to the accurate identification of OAM modes. Furthermore, the validity and efficiency of this method are confirmed through an example and some simulations analysis, such as the comparison of analog devices, the identification probability, BER and the capacity. The simulation results also show that the BER performance of this method can be improved by 4 dB and the transmission distance can be extended, e.g., from 100 km to 158.4 km. Moreover, with the incoming of the next generation mobile communications (B5G and 6G), aimed at the problem of OAM mode identification in the long distance and low SNR transmission, the wireless high-speed transmission even to 1 Tbps with the low sampling rate becomes a promising topic. Evidently, it can be predicted that the proposed method is significant to promote the transmission distance and the transmission capacity with the intelligent low sampling rate AIC hardware equipment in the future.

Furthermore, it has to be admitted that, although a scenario in the multipath effect transmission channel with the constant attenuation and randomly varying delays within a certain range can be established by transfer learning, the actual multipath environment may be more complicated, and the current neural network datasets are very limited and can only be regarded as small sample datasets. In order to ensure the high accuracy and satisfy the actual scenarios, more diverse datasets need to be trained and a large number of practical field tests to get more data in different real transmission scenarios for training should be carried out. Moreover, in the actual transmission multipath environment, the network structure has to be continuously optimized, and there is still amount of work to be done later.

Acknowledgments

This work is supported in part by the Science and Technology Key project of Guangdong Province with project number 2019B010157001, in part by the National Natural Science Foundation of China with project number 61731011, the Industrial Interconnection Platform Project of Ministry of Industry and Information Technology with project number 20201660184, and ZTE Industry-University-Research Cooperation Forum with project number 2018ZTE01-01-03.

References

[1] F. L. Luo, Signal Processing Techniques for 5G: An Overview, *ZTE Communications*, No. 1, pp. 24-31, April, 2015.

[2] Y. Xu, X. Wu, G. Yang, N. Chi, Fiber-wireless Integrated Reliable Access Network for Mobile Fronthaul using Synclastic Uniform Circular Array with Dual-mode OAM

Multiplexing, *ZTE Communications*, No. 4, March, 2020.

[3] E. Basar, Orbital Angular Momentum with Index Modulation, *IEEE Transactions on Wireless Communications*, Vol. 17, No. 3, pp. 2029-2037, March, 2018.

[4] C. Zhang, L. Ma, Millimetre Wave with Rotational Orbital Angular Momentum, *Scientific Reports*, Vol. 6, p. 31921, September, 2016.

[5] W. Zhang, S. Zheng, Y. Chen, X. Jin, H. Chi, X. Zhang, Orbital Angular Momentum-Based Communications with Partial Arc Sampling Receiving, *IEEE Communications Letters*, Vol. 20, No. 7, pp. 1381-1384, July, 2016.

[6] Y. Zhao, J. Jiang, X. Jiang, C. Zhang, Orbital Angular Momentum Multiplexing with Non-Degenerate Modes in Secondary Frequency Domain, *IEEE MTT-S International Wireless Symposium (IWS)*, Chengdu, China, 2018, pp. 1-4.

[7] C. Zhang, L. Ma, Detecting the Orbital Angular Momentum of Electro-Magnetic Waves Using Virtual Rotational Antenna, *Scientific Reports*, Vol. 7, No. 1, p. 4585, July, 2017.

[8] C. Zhang, D. Chen, X. Jiang, RCS Diversity of Electromagnetic Wave Carrying Orbital Angular Momentum, *Scientific Reports*, Vol. 7, No. 1, p. 15412, November, 2017.

[9] C. Zhang, Y. Zhao, Orbital Angular Momentum Nondegenerate Index Mapping for Long Distance Transmission, *IEEE Transactions on Wireless Communications (TWC)*, Vol. 18, No. 11, pp. 5027-5036, November, 2019.

[10] H. Gao, Y. Duan, L. Shao, X. Sun, Transformation-based Processing of Typed Resources for Multimedia Sources in the IoT Environment, *Wireless Networks*, Vol. 26, pp. 1-17, November, 2019.

[11] H. Gao, Y. Xu, Y. Yin, W. Zhang, R. Li, X. Wang, Context-Aware QoS Prediction with Neural Collaborative Filtering for Internet-of-Things Services, *IEEE Internet of Things Journal*, Vol. 7, No. 5, pp. 4532-4542, May, 2020.

[12] H. Gao, C. Liu, Y. Li, X. Yang, V2VR: Reliable Hybrid-Network-Oriented V2V Data Transmission and Routing Considering RSUs and Connectivity Probability, *IEEE Transactions on Intelligent Transportation Systems(T-ITS)*, pp. 1-14, April, 2020.

[13] D. L. Donoho, Compressed Sensing, *IEEE Transactions on Information Theory*, Vol. 52, No. 4, pp. 1289-1306, April, 2006.

[14] W. Ding, F. Yang, W. Dai, J. Song, Time-Frequency Joint Sparse Channel Estimation for MIMO-OFDM Systems, *IEEE Communications Letters*, Vol. 19, No. 1, pp. 58-61, January, 2015.

[15] C. Zhou, Y. Gu, Y. D. Zhang, Z. Shi, T. Jin, X. Wu, Compressive Sensing-Based Coprime Array Direction-of-Arrival Estimation, *IET Communications*, Vol. 11, No. 11, pp. 1719-1724, August, 2017.

[16] J. Jiang, C. Chen, Analysis in Theory and Technology Application of Compressive Sensing, 2*014 Sixth International Conference on Intelligent Human-Machine Systems and Cybernetics*, Hangzhou, China, 2014, pp. 184-187.

[17] L. He, J. Wang, W. Ding, J. Song, Minimization Based Symbol Detection for Generalized Space Shift Keying, *IEEE Communications Letters*, Vol. 19, No. 7, pp. 1109-1112, July, 2015.

[18] C. M. Yu, S. H. Hsieh, H. W. Liang, C. S. Lu, W. H. Chung, S. Y. Kuo, S. C. Pei, Compressed Sensing Detector Design for Space Shift Keying in MIMO Systems, *IEEE Communications Letters*, Vol. 16, No. 10, pp. 1556-1559, October, 2012.

[19] W. Liu, N. Wang, M. Jin, H. Xu, Denoising Detection for the Generalized Spatial Modulation System Using Sparse Property, *IEEE Communications Letters*, Vol. 18, No. 1, pp. 22-25, January, 2014.

[20] C. Zhang, Z. Wu, J. Xiao, Adaptive Analog-to-Information Converter with Limited Random Sequence Modulation, *2011 International Conference on Wireless Communications and Signal Processing (WCSP)*, Nanjing, China, 2011, pp. 1-5.

[21] L. Kuang, X. Yan, X. Tan, S. Li, X. Yang, Predicting Taxi Demand Based on 3D Convolutional Neural Network and Multi-task Learning, *Remote Sensing*, Vol. 11, No. 11, p. 1265, May, 2019.

[22] J. Yu, J. Li, Z. Yu, Q. Huang, Multimodal Transformer with Multi-View Visual Representation for Image Captioning, *IEEE Transactions on Circuits and Systems for Video Technology*, pp. 1-1, October, 2019.

[23] T.-L. Lin, H.-Y. Chang, K.-H. Chen, The Pest and Disease Identification in the Growth of Sweet Peppers Using Faster R-CNN and Mask R-CNN, *Journal of Internet Technology*, Vol. 21, No. 2, pp. 605-614, March, 2020.

[24] X. Ma, H. Ye, Y. Li, Learning Assisted Estimation for Time-Varying Channels, *2018 15th International Symposium on Wireless Communication Systems (ISWCS)*, Lisbon, Portugal, 2018, pp.1-5.

[25] H. Ye, G. Y. Li, B. Juang, Power of Deep Learning for Channel Estimation and Signal Detection in OFDM Systems, *IEEE Wireless Communications Letters*, Vol. 7, No. 1, pp. 114-117, August, 2017.

[26] E. M. Knutson, S. Lohani, O. Danaci, S. D. Huver, R. T. Glasser, Deep Learning as a Tool to Distinguish between High Orbital Angular Momentum Optical Modes, *Optics & Photonics for Information Processing X.*, Vol. 9970, pp. 236-242, September, 2016.

[27] A. T. Watnlk, T. Doster, Measuring Multiplexed OAM Modes with Convolutional Neural Networks, *Applications of Lasers for Sensing and Free Space Communications*, Boston, American, 2016, paper LTh3B.2.

[28] T. Doster, A. T. Watnlk, Machine Learning Approach to OAM Beam Demultiplexing Via Convolutional Neural Networks, *Applied Optics*, Vol. 56, No. 12, pp. 3386-3396, July, 2017.

[29] S. J. Pan, Q. Yang, A Survey on Transfer Learning, *IEEE Transactions on Knowledge and Data Engineering*, Vol. 22, No. 10, pp. 1345-1359, October, 2010.

[30] J. A. Tropp and A. C. Gilbert, Signal Recovery from Random Measurements Via Orthogonal Matching Pursuit, *IEEE Transactions on Information Theory*, Vol. 53, No. 12, pp. 4655-4666, December, 2007.

[31] J. Yu, C. Zhu, J. Zhang, Q. Huang, D. Tao, Spatial Pyramid-Enhanced NetVLAD with Weighted Triplet Loss for Place

Recognition, *IEEE Transactions on Neural Networks and Learning Systems*, Vol. 31, No. 2, pp. 661-674, February, 2020.

[32] A. Krizhevsky, I. Sutskever, G. Hinton, ImageNet Classification with Deep Convolutional Neural Networks, *Advances in Neural Information Processing Systems 25 (NIPS 2012)*, Lake Tahoe, Nevada, USA, 2012, pp. 1097-1105.

[33] J. D. Jackson, *Classical Electrodynamics*, Wiley, 1999.

[34] W. Zhang, S. Zheng, X. Hui, R. Dong, X. Jin, H. Chi, X. Zhang, Mode Division Multiplexing Communication Using Microwave Orbital Angular Momentum: An Experimental Study, *IEEE Transactions on Wireless Communications*, Vol. 16, No. 2, pp. 1308-1318, February, 2017.

[35] X. Jiang, Y. Zhao, X. Jiang and C. Zhang, Capacity Evaluation on the Long-Distance Orbital Angular Momentum Non-Orthogonal Transmission, *IEEE MTT-S International Wireless Symposium (IWS)*, Chengdu, China, 2018, pp. 1-4.

[36] L. Shao, F. Zhu, X. Li, Transfer Learning for Visual Categorization: A Survey, *IEEE Transactions on Neural Networks and Learning Systems*, Vol. 26, No. 5, pp. 1019-1034, May, 2015.

Biographies

Chao Zhang received the B.E. degree from Xi'an Jiaotong University, Xi'an, China, in 2000, the M.E. and D.Eng. degrees from Tsinghua University, Beijing, China, in 2002 and 2005, respectively. Meanwhile, he was selected in the Joint Doctoral Program of the State Key Laboratories of China and Japan, and received the Ph.D. degree from the National Institute of Informatics, SOKENDAI, Tokyo, Japan, in 2006. Since 2005, he has been a Faculty Member of the Labs of Avionics, School of Aerospace Engineering, Tsinghua University, Beijing. So far, his research topics concentrate on the electromagnetic wave transmission with Orbital Angular Momentum (OAM), OAM quantum vortex, OAM radar, and avionics systems. He is an IET Fellow, an IEEE Senior Member, and an IEICE Senior Member.

Jin Li received the B.E. degree in Automation from Beijing University of Technology, Beijing, China, in 2017, and the M.E. degree from School of Aerospace Engineering, Tsinghua University, Beijing, China, in 2020. His research interests include Orbital Angular Momentum (OAM) transmission and magnetic positioning with high accuracy.

Yuanhe Wang is pursuing Ph.D. in Labs of Avionics, School of Aerospace Engineering, Tsinghua University, Beijing, China. He received the B.E. degree in Communication Engineering from Xidian University, Xi'an, China. His research focuses on the transmission of Orbital Angular Momentum (OAM).